Carbohydrate Recognition in the Peripheral Nervous System: A Calcium-dependent Membrane Binding Site for HNK-1 Reactive Glycolipids Potentially Involved in Schwann Cell Adhesion

Leila K. Needham and Ronald L. Schnaar

Departments of Pharmacology and Neuroscience, The Johns Hopkins University School of Medicine, Baltimore, Maryland 21205

Abstract. The carbohydrate determinants recognized by the HNK-1 antibody are potential cell–cell recognition ligands in the peripheral nervous system (PNS). The HNK-1 reactive sulfoglucuronylneolacto (SGNL) glycolipids specifically support Schwann cell adhesion, suggesting the presence of a cell surface receptor specific for SGNL-oligosaccharides. We directly probed PNS membranes for receptors complementary to SGNL determinants using a synthetic radioligand consisting of radioiodinated serum albumin derivatized with multiple SGNL-oligosaccharides. A high-affinity, saturable, calcium-dependent binding site for this ligand was found in PNS myelin membranes. Binding activity was carbohydrate-specific (most potently inhibited by SGNL-lipids compared to other glycolipids) and PNS-specific (absent from comparable central nervous system membranes). The SGNL-specific binding activity on PNS membranes reported here may be involved in peripheral myelination or myelin stabilization.

RECENTLY, unusual carbohydrate determinants recognized by the HNK-1 mAb and the monoclonal L2 antibodies have been proposed to function in neural recognition, perhaps as adhesive determinants (9, 26, 47). HNK-1 reactive species include a unique class of anionic glycosphingolipids, the sulfoglucuronylneolacto-lipids (SGNL-lipids)[1], in addition to undefined, but presumably related, carbohydrate determinants on minor glycoforms of adhesive glycoproteins including NCAM, MAG, P_o, L1, and J1/cytotactin (50). Consistent with a role in cell recognition, HNK-1 and L2 mAbs attenuate cell adhesion in several neural cell model systems in vitro (9, 26, 47). The observation that SGNL-lipids and SGNL-oligosaccharides perturb cell–cell and cell–substratum adhesion in vitro provides more direct evidence for a role of these HNK-1 reactive oligosaccharides as authentic adhesive ligands (29).

Further evidence for an adhesive role for SGNL-determinants comes from clinical studies. SGNL-lipids were first identified as antigens of monoclonal IgM's produced by a majority of patients with peripheral demyelinating neuropathy associated with IgM paraproteinemia (excess production of monoclonal IgM). These IgM paraproteins exhibit carbohydrate structural specificities similar to the HNK-1 and L2 antibodies (45, 62). The two major structurally characterized SGNL-lipids are closely related and consist of a nonreducing terminal glucuronic acid 3-sulfate attached (β1-3) to the terminal galactose of neolactotetraosylceramide or neolactohexaosylceramide (1, 6). SGNL-lipids are found in the adult peripheral nervous system (PNS) of many species (7, 23), but are not detected in adult cerebral cortex, although they are expressed in embryonic cortex and in adult cerebellum (8, 43). In the PNS, subcellular fractionation has localized SGNL-lipids to the axolemma-enriched fraction, as well as myelin and other Schwann cell membranes (27).

We have focused on the possible role of the SGNL-lipids as adhesive ligands recognized by Schwann cell surface receptors. The initial impetus for pursuing this hypothesis arose from the following observations. (*a*) The pathology and morphological changes in the subclass of patients with peripheral demyelinating neuropathy associated with a SGNL-lipid reactive IgM paraprotein is consistent with a disruption of Schwann cell surface interactions necessary for myelin maintenance or myelination (44, 53). (*b*) SGNL-lipids are present in the membranes of axons and Schwann cells (27), and are therefore in the proper location to mediate axon-Schwann cell or myelin lamellae–lamellae interactions. (*c*) SGNL-lipids and SGNL-oligosaccharides are capable of inhibiting neural cell–cell and cell–substratum interactions in vitro (29). (*d*) There is a growing body of evidence that glycosphingolipids may function as determinants in cell–cell interactions involved in leukocyte and platelet adhesion to vascular endothelium and in neural cell recognition (3, 17, 51). In particular, the demonstration of a carbohydrate-specific ganglioside binding protein that is present in central nervous system (CNS) but not PNS myelin and which may be involved in oligodendrocyte–axon interactions (58, 59) raised the possibility that another class of anionic glycosphingolipids, the SGNL-lipids, may be playing a similar role in PNS myelin. More-

1. *Abbreviations used in this paper*: CNS, central nervous system; CMF-PBS, divalent cation-free phosphate buffered saline; PNS, peripheral nervous system; SGNL, sulfoglucuronylneolacto.

over, our previous studies demonstrated Schwann cell adhesion directly and selectively to SGNL-lipids, using a technique which detects adhesion of intact cells directly to chromatographically resolved lipids (57). When peripheral nerve lipids were resolved by TLC and overlaid with radiolabeled Schwann cells, the SGNL-lipids supported cell adhesion with greater potency than any other PNS lipids (38). The adhesion was cell type specific in that neither hepatocytes, fibroblasts, nor retina cells adhered to the SGNL-lipids (39). These data suggest the presence of a Schwann cell surface receptor specific for the SGNL-oligosaccharide.

To probe directly for the presence of a SGNL-oligosaccharide receptor in the PNS, we constructed a multivalent radioligand consisting of SGNL-oligosaccharides covalently attached to a radioiodinated carrier protein, BSA. Through the use of this ligand, we now report the properties of a complementary SGNL-specific binding site on PNS myelin.

Materials and Methods

SGNL-lipid Purification

SGNL-lipids were purified from dog sciatic nerve endoneurium (Pel-Freeze Biologicals, Rogers, AR), from bovine cauda equina (obtained at time of slaughter), or from human cauda equina (obtained at autopsy or kindly provided by the National Neurological Research Specimen Bank, Los Angeles, CA) using modifications of published procedures (1, 6). Tissue (~100 g wet weight, stored at −70°C before use) was thawed, homogenized in a Polytron high-speed motor-driven homogenizer (dog and bovine tissue) or a Waring blender (human tissue), and extracted sequentially with 15 and 7.5 vol (relative to the original tissue wet weight) chloroform/methanol/water (4:8:3) ([56]; all solvent ratios are vol/vol). Precipitated protein was removed by centrifugation, and the supernatant evaporated to dryness. The resulting residue was extracted by incubation in 4 vol of chloroform/methanol (1:1) for ~16 h at 4°C. The remaining solids were recovered by centrifugation and dissolved in 2.5 vol of chloroform/methanol/water (4:8:3). After removal of the remaining precipitate by centrifugation, water was added to a final ratio of chloroform/methanol/water of 4:8:5.6 (56). The resulting upper aqueous phase was readjusted to chloroform/methanol/water (4:8:3) and applied to a column (0.25 vol relative to original tissue weight) of DEAE-Sepharose Fast Flow (acetate form, Pharmacia LKB Biotechnology Inc., Piscataway, NJ) equilibrated in the same solvent. The column was eluted with 2 column vol of the starting solvent, 8 column vol of methanol, 4 column vol of 0.04 M ammonium acetate in methanol, and 4 column vol of 0.1 M ammonium acetate in methanol to elute phospholipids, sulfatides, and gangliosides (18, 35). The SGNL-lipids were then eluted with 10 column vol of 0.2 M ammonium acetate in methanol. This fraction was concentrated on a vacuum rotary evaporator (Rotovap, Büchi), diluted with water, and dried on a vacuum centrifugal evaporator (Speedvac, Savant) to remove volatile salts. The residue was dissolved in 8 ml chloroform: methanol/water (70:30:4), and applied to a 1-ml column of Iatrobeads silicic acid (Iatron Laboratories, Tokyo, Japan). The column was washed with 6 ml chloroform/methanol/water (70:30:4), and SGNL-lipids were eluted in 2 ml chloroform/methanol/water (60:35:8) followed by 4 ml of 10:10:3. The latter two fractions were pooled, evaporated, and dissolved in chloroform/methanol/water (2:43:55), and applied to two prewashed C18 Sep-Pak cartridges (Waters) in tandem (60). The cartridges were washed with 16 ml water, 8 ml methanol/water (2:1), and then SGNL-lipids were eluted with 16 ml methanol/water (4:1) and 8 ml methanol. The purified SGNL-lipids were pooled, solvents evaporated, and the residue dissolved in chloroform/methanol/water (4:8:3) for storage.

The purification of the SGNL-lipids was monitored by TLC on silica gel HPTLC plates (E. Merck, Darmstadt, FRG) using chloroform/methanol/0.25% KCl (60:35:8) as developing solvent and a variety of lipid stains to detect contaminating glycolipids and phospholipids including resorcinol (specific for gangliosides [12, 55]), *N*-1-napthylethylenediamine dihydrochloride (specific for sugars [2]), Azure A (specific for sulfated compounds [22]), and cupric sulfate/phosphoric acid char (nonspecific lipid stain [61]). In the purified SGNL-lipid fraction (from all three species), two major components were detected with *N*-1-napthyl-ethylenediamine, Azure A, and cupric sulfate/phosphoric acid: the most abundant species (60–90% depending on the species, R_f = 0.20–0.24), and a less abundant species (10–35%, R_f = 0.09–0.14). In addition, a third species of low abundance (~5%, R_f = 0.05) was detected with these three stains in the purified SGNL-lipid fraction derived from bovine cauda equina. No resorcinol positive material was detected in these fractions. The three species were also detected with HNK-1 antibody and the two faster migrating species comigrated with authentic $SGNL_4$- and $SGNL_6$-lipids (kindly provided by Dr. Robert Yu, Virginia Commonwealth University, Richmond, VA). The HNK-1 immuno-overlay procedure was modified from the procedure of Magnani (35) as follows. After resolution of the lipids by HPTLC, the TLC plates were dried at 50°C for 1 h, and then treated for 30 s sequentially with hexane and with 0.01% poly(isobutylmethacrylate) (Aldrich Chem. Co., Milwaukee, WI) in hexane, after which they were dried under a stream of air. After the plates were prewet by spraying with divalent cation-free phosphate buffered saline (CMF-PBS) (16), they were incubated for ~16 h at 4°C with HNK-1 antibody (Leu-7, Becton Dickinson, Mountain View, CA) at a dilution of 1 μg/ml in CMF-PBS containing 0.2% BSA. The TLC plate was washed by transfer into CMF-PBS and bound antibody localized by incubation of the plate with biotinylated goat anti-mouse IgM and with avidin/biotinylated horseradish peroxidase complex (Vector Labs, Inc., Burlingame, CA) diluted in CMF-PBS, followed by peroxidase detection using diaminobenzidine as substrate according to the manufacturer's instructions for processing nitrocellulose blots.

The concentration of SGNL-lipids was determined by quantitative TLC in the above solvent system and 2% Azure A in 1 mM sulfuric acid to stain sulfated compounds (22). Sulfatides were used as quantitative standards. Alternatively, the concentration of SGNL-lipids was determined by saccharide compositional analysis using a Dionex HPLC carbohydrate analysis system (see below). The two methods yielded essentially identical results. In addition, SGNL-lipids were characterized by fast atom bombardment MS (see below).

Synthesis of ^{125}I-SGNL-BSA

SGNL-oligosaccharide was released from the parent lipid using ceramide glycanase (V-Labs, Covington, LA) under conditions described previously (63). The optimal procedure is as follows. SGNL-lipid (2.6 μmol) isolated from dog sciatic nerve endoneurium was treated with 17 U ceramide glycanase for 24 h at 37°C in 6.5 ml 50 mM sodium acetate buffer, pH 5.0, containing 0.75 mg/ml sodium cholate. The reaction was stopped by the addition of 19.5 ml of acetonitrile/water (1:2) and the solution passed over two C18 reverse phase cartridges in tandem to remove detergent and ceramide (6).

The purified SGNL-oligosaccharide was conjugated to BSA by reductive amination using pyridine borane as reducing reagent (4). SGNL-oligosaccharide (~2 μmol) was added in ~50-fold molar excess to 2.7 mg BSA (essentially fatty acid- and globulin-free, Sigma Chem. Co., St. Louis, MO) in 320 μl of 0.1 M sodium phosphate buffer, pH 7.0. Methanol and pyridine borane (40 μl each) were added and the reaction was allowed to proceed for 5.5 d at 50°C under nitrogen. Analysis of the reaction mixture by silica gel HPTLC (E. Merck) using *n*-butanol/acetic acid/water (2:1:1) as the developing solvent and 13 mM *N*-(1-napththyl)ethylenediamine dihydrochloride in 3% sulfuric acid in methanol to visualize sugars (2) revealed the disappearance of the two oligosaccharide bands (R_f's = 0.11 and 0.05), and a concomitant increase in saccharide-positive material at the origin, as expected for saccharides conjugated to protein. The reaction mixture was extracted with ethyl acetate to remove pyridine borane and SGNL-BSA was purified by gel permeation chromatography on Sephadex G-25 and anion exchange HPLC on a Beckman DEAE (5PW) column, as described (58). Purified SGNL-BSA was radioiodinated using $Na^{125}I$ (Amersham Corp., Arlington Heights, IL) and Iodobeads (Pierce Chem. Co. Rockford, IL) as previously described (58) to initial specific activities of 200–600 Ci/mmol.

^{125}I-SGNL-BSA Characterization

^{125}I-SGNL-BSA was subjected to gradient SDS-polyacrylamide electrophoresis (31) as follows. Aliquots of ^{125}I-SGNL-BSA (~100 fmol) were boiled in sample buffer containing SDS and β-mercaptoethanol and loaded onto a 10–20% gradient polyacrylamide mini-gel (Integrated Separation Sys., Natick, MA). Electrophoresis was conducted at 40 milliamps constant current on a Hoeffer Mighty Small II apparatus. The gel was blotted onto nitrocellulose in using a BioRad "Transblot" electrophoretic transfer apparatus. After transfer in 25 mM Tris base 192 mM glycine 20% methanol for 3 h at 70 V, the blot was dried and exposed to X-ray film to obtain an autoradiographic image, and then processed for HNK-1 reactive oligosaccharide immunolocalization. The blot was preincubated with 3% BSA in 10 mM Tris buffer, pH 7.4, containing 15 mM NaCl, and then incubated with

HNK-1 antibody (Leu-7, Becton Dickenson) at a dilution of 1 μg/ml in CMF-PBS containing 0.2% BSA. The blot was washed by transfer into CMF-PBS and bound antibody localized by incubation of the blot with biotinylated goat anti-mouse IgM and with avidin/biotinylated horseradish peroxidase complex (Vector Labs) diluted in CMF-PBS, followed by peroxidase detection using diaminobenzidine as substrate according to the manufacturer's instructions.

Carbohydrate compositional analysis was performed by anion exchange chromatography with pulsed amperometric detection on a Dionex BioLC HPLC system. The glucuronic acid was converted to glucose (24) before hydrolysis as follows. An aliquot of SGNL-BSA (924 pmol) or SGNL-lipid (~1 nmol) was evaporated in a test tube and the residue treated with 100 μl anhydrous 0.05 N HCl in methanol for 4 h at ambient temperature to produce the desulfated glucuronyl-methyl ester. Sodium borate buffer, pH 9 (0.2 N, 10 μl), NaOH (0.5 N, 10 μl), and sodium borohydride in methanol (20 mg/ml, 100 μl) were added to reduce the glucuronyl-methyl ester to glucose. After ~16 h at ambient temperature, excess sodium borohydride was destroyed by the addition of 30 μl 2 N acetic acid. The resulting mixture was evaporated to dryness. The residue was hydrolyzed in 200 μl 2 N trifluoroacetic acid for 5 h at 100°C to release monosaccharides. Samples were evaporated to dryness under a stream of nitrogen, dissolved in 250 μl of water, and 50 μl aliquots were injected on a Dionex HPIC AS6 column. Procedures for elution and pulsed amperometric detection for quantitation of monosaccharides were as previously described (33).

SGNL-BSA protein values were determined by densitometry of Amido Black stained nitrocellulose slot blots of protein aliquots, using the procedure of Sailer and Weissmann (48) modified as follows. Aliquots (100 μl) containing 0.1–1.2 μg BSA standard or unknown sample were placed in 96-well polystyrene microplate wells. SDS (10%, 10 μl) was added, the plate incubated for 5 min at ambient temperature, 67 μl of 50% trichloroacetic acid was added, and the plate was incubated for an additional 5 min. The contents of each well were transferred to nitrocellulose filters using a Minifold II slot-blot apparatus (Schleicher and Schuell, Inc., Keene, NH). Each sample application slot was washed with two aliquots (200 μl) of 6% trichloroacetic acid, the nitrocellulose filter was removed from the manifold, stained for 3 min in 0.1% Amido Black 10B in methanol/water/acetic acid (45:45:10), washed in water for 1 min, destained in methanol/water acetic acid (90:8:2) for 3 min, and washed in water for 1 min. Protein stain was quantitated using a Kontes Fiber Optic Scanner.

SGNL-BSA and parent BSA were also analyzed by laser desorption mass spectroscopy (5), which was kindly performed by Drs. Robert Cotter and Marc Chevrier of the Middle Atlantic Mass Spectrometry Laboratory, an NSF Regional Instrumentation Facility, Baltimore, MD.

Peripheral Nerve Endoneurium Subcellular Fractionation

Rat sciatic nerve myelin was prepared according to modifications of the methods of Oulton and Mezei (42) by Tiemeyer et al. (59). Rat sciatic nerve endoneurium was dissected from rat sciatic nerve (Pel-Freeze) in CMF-PBS, the endoneurium was collected by centrifugation, resuspended in 0.29 M sucrose, and stored at −70°C until use. Thawed endoneurium (~2 g, from 125 nerves) was homogenized in 20 ml of 0.29 M sucrose using a Polytron tissue disruptor and the homogenate was centrifuged at 1,000 *g* for 10 min to remove nondisrupted tissue, unbroken cells, and nuclei, yielding a crude supernatant "S1" fraction. In some experiments, a small portion of the S1 fraction was centrifuged (72,000 *g*, 45 min), and the pellet was resuspended in 1 ml 0.29 M sucrose, diluted 10-fold with 10 mM EGTA in 1 mM Hepes, pH 7.5, and recentrifuged. The resulting pellet was resuspended in a small volume of 0.29 M sucrose to yield the mixed membrane "P2" fraction. The remainder of S1 was diluted to 24 ml with 0.29 M sucrose and 12 ml were overlaid onto each of two discontinuous sucrose gradients consisting of 10 ml 0.8 M sucrose over 10 ml 1.2 M sucrose. The gradients were centrifuged at 72,000 *g* for 2.5 h in a swinging bucket ultracentrifuge rotor. The material banding at each of the 0.29/0.8 M and 0.8/1.2 M sucrose interfaces was collected with a pasteur pipette in ~6 ml vol, diluted to 36 ml with 10 mM EGTA in 1 mM Hepes, pH 7.5, and recentrifuged at 72,000 *g* for 45 min. The pellets from the 0.29/0.8 M sucrose interfaces and from 0.8/1.2 M sucrose interfaces were resuspended in small volumes of 0.29 M sucrose to yield a myelin enriched fraction, S1A (from the material forming a compact white band at the 0.29/0.8 M sucrose interface), and a denser mixed membrane fraction, S1B (from the material forming a diffuse off-white band at the 0.8/1.2 M sucrose interface). In some experiments, a portion of the S1A fraction was further subjected to osmotic shock and homogenization and purified by subjecting it to a second discontinuous sucrose gradient centrifugation as follows. As aliquot (~3 ml) of the S1A fraction was diluted with 10 vol of 10 mM EGTA in 1 mM Hepes, pH 7.5, homogenized manually (glass teflon, 5 strokes), and incubated on ice for 15 min. After centrifugation at 72,000 *g* for 45 min, the pellet was resuspended in 6 ml 0.29 M sucrose with trituration and brief homogenization, and resubjected to discontinuous sucrose gradient as described above, except that only the material banding at the 0.29/0.8 M sucrose interface was collected by centrifugation and resuspended in a small volume of 0.29 M sucrose to yield a purified myelin fraction, S2. All fractions were stored frozen in small aliquots before use. Protein content was determined using the bicinchoninic acid assay (52) with BSA as a standard.

Central Nervous System Tissue Subcellular Fractionation

Crude membrane fractions (P2) were prepared from whole rat brain and from cerebellum (cerebellar P2) by the differential centrifugation method of Cotman (11) as previously described (59). Fractions enriched in myelin (P2A) and in synaptosomes (P2B) were prepared from whole rat brain by the discontinuous sucrose gradient centrifugation method of Gray and Whittaker (19) as previously described (59).

^{125}I-SGNL-BSA Binding to Membranes

An aliquot of membranes containing 0.1–10 μg protein in 25 μl of 0.29 M sucrose was added to 225 μl of binding buffer (50 mM imidazole acetate, pH 7.4, 0.032% Triton X-100 (Surfact-Amps X-100, Pierce Chem. Co.), 1 mg/ml BSA (Fraction V, Sigma Chem. Co.), and 20 mM $CaCl_2$ containing 0.5 nM ^{125}I-SGNL-BSA (or as indicated). The reaction tubes were agitated, and then incubated on a shaker at 4°C for 30 min (or as indicated). When lipids were added as inhibitors, they were evaporated from organic solvent stock solutions under a stream of nitrogen and the residue resuspended by bath sonication in 50 mM imidazole acetate, pH 7.4, containing 0.032% Triton X-100 before appropriate dilution into binding buffer. For all inhibition studies, membranes were preincubated in binding buffer containing inhibitors for 30 min at 4°C before addition of radioligand and incubation for an additional 30 min. Subsequent to incubations, membrane-bound radioligand was separated from free ligand by filtration over glass fiber filters (Schleicher and Schuell, Inc.) using a Brandel Cell Harvester. The filters were pretreated with 1% BSA in water to reduce background binding and were rinsed with 50 mM imidazole acetate, pH 7.4, before use. After filtration of the binding reactions, the filters were washed three times, ~3 ml each, with ice cold 50 mM imidazole acetate, pH 7.4. Radioactivity remaining on the filter was measured using a γ-radiation counter. Nonspecific binding was determined in the absence of $CaCl_2$ or of membranes, as indicated.

Lipid and Anionic Saccharide Inhibitors

Sulfatide and globotetraosylceramide were obtained from Matreya, Inc. (Chelfont, PA); cholesterol-3′-sulfate, galactosylceramide, and anionic saccharides (except SGNL-oligosaccharide, see above) from Sigma Chem. Co.; phospholipids were obtained from Avanti Polar Lipids (Birmingham, AL) or from Sigma Chem. Co.; and individual purified bovine brain gangliosides were obtained either from Sigma Chem. Co. or E-Y Laboratories (San Mateo, CA). Synthetic 2,3 sialyl- and 2,6 sialyl Lewis x glycolipids (25) were prepared by Dr. A. Hasegawa, Department of Applied Organic Chemistry, Gifu University, Japan, and were kindly provided by Dr. Brian Brandley, Glycomed, Inc., Alameda, CA. Sialylneolactotetraosylceramides were kindly provided by Paul James, Glycomed, Inc., Alameda, CA.

Desulfated SGNL-lipid and its methyl ester were prepared by chemical modification of human cauda equina SGNL-lipids by the method of Chou et al. (6). The purity and the concentrations of the products were determined by quantitative TLC on silica gel HPTLC plates (E. Merck) using chloroform/methanol/0.25% KCl as developing solvent, cupric sulfate/phosphoric acid char (61) for detection, and the parent SGNL-lipid as a standard for quantitation. Each derivative appeared as a single major species which migrated distinctly from the parent SGNL-lipid. The R_f values were as follows: Parent lipid (predominantly IV^{3}glucuronylneolactotetraosylceramide V^3-sulfate), 0.35; desulfated SGNL-lipid (IV^{3}glucuronylneolactotetraosylceramide), 0.39; and methyl esterified desulfated SGNL-lipid (IV^{3}glucuronylneolactotetraosylceramide V^6-methyl ester), 0.59. The identity of each lipid was confirmed by fast atom bombardment mass spectroscopy in the negative ion mode using a Finnigan MAT 900 spectrometer with triethylamine as matrix as kindly performed by Dr. Hans Schweingruber, Glycomed, Inc., Alameda, CA. Characteristic of glycosphingolipids (20), the

parent SGNL-lipid produced a family of molecular ions representing heterogeneity in the ceramide (lipid) moiety, with the major molecular ion (M-1) at 1593, corresponding to a ceramide composed of C_{18} sphingosine and a $C_{24:0}$ fatty acid amide as previously reported (6). The major molecular ion (M-1) generated by the desulfated species was 1513, as expected, and the methyl ester generated the same molecular species (M-CH_3) as well as the molecular ion (M-1) at 1527 (24).

Results

SGNL-derivatized Radioligand Synthesis and Characterization

A polyvalent SGNL-derivatized radioligand was prepared by covalently linking SGNL-oligosaccharides enzymatically released from SGNL-lipids to a carrier protein, BSA. To this end, efficient methods for the purification of SGNL-glycolipids from peripheral nerve and the production of SGNL-oligosaccharides were developed. Dog sciatic endoneurium was chosen as the tissue source because of its relatively high abundance of SGNL-lipid (23). The procedure for the purification of SGNL-lipids was based upon the unexpected observation that these highly polar lipids are differentially insoluble in chloroform/methanol (1:1). When a chloroform/methanol/water (4:8:3) lipid extract from dog sciatic endoneurium was evaporated to dryness and the residue reextracted with chloroform/methanol (1:1), ~98% of the neutral lipids, phospholipids, and glycolipids (including gangliosides) were solubilized (30), while ~70% of the SGNL-lipids were recovered in the insoluble residue. The SGNL-lipids were further purified from lipid and polypeptide contaminants by partitioning, DEAE-Sepharose chromatography, silicic acid chromatography, and reserve-phase chromatography to yield ~2.6 μmol of SGNL-lipids from 100 g (wet weight) of dog sciatic nerve endoneurium. Purified SGNL-lipids consisted of two major species, resolved by TLC, which correspond to the previously described (1,6) closely related structures IV^{3}glucuronylneolactotetraosylceramide V^3-sulfate ($SGNL_4$-lipid, 60%) and VI^{3}glucuronylneolactohexaosylceramide VII^3-sulfate ($SGNL_6$-lipid, 40%) (Fig. 1). These species comigrated with known standards (kindly provided by Dr. Robert Yu, Virginia Commonwealth University, Richmond, VA) and were reactive with HNK-1 antibody (data not shown).

Treatment of the SGNL-lipids with leech ceramide glycanase (63) resulted in essentially complete conversion of the SGNL-lipids to the corresponding SGNL-oligosaccharides and ceramide. The oligosaccharides were purified by reverse-phase chromatography and the purity of the products was confirmed by silica gel TLC developed in *n*-butanol/acetic acid/water (2:1:1). The oligosaccharides were detected as two species which migrated slower than the parent lipid species ($SGNL_4$-lipid R_f = 0.49, $SGNL_6$-lipid R_f = 0.28, $SGNL_4$-oligosaccharide R_f = 0.11, $SGNL_6$-oligosaccharide R_f = 0.05) (data not shown). The SGNL-oligosaccharides were coupled to BSA by reductive amination, and the resulting SGNL-BSA conjugate was purified by DEAE-HPLC and gel filtration chromatography. The SGNL-BSA was labeled to high specific activity with $Na^{125}I$ for use as a radioligand (subsequent to labeling, 5 mg/ml of underivatized BSA was added to protect against radiation-induced damage).

The derivatization ratio of the SGNL-BSA conjugate was determined by hydrolysis and saccharide analysis. Since the glucuronic acid–galactose glycosidic linkage is resistant to hydrolysis, the conjugate was hydrolyzed after methyl esterification and reduction of the glucuronic acid to glucose. Control hydrolysis of SGNL-lipids treated under identical conditions in the presence of underivatized BSA resulted in a galactose recovery which was 98% of theoretical. Saccharide analysis of the hydrolyzed SGNL-BSA conjugate yielded ratios of galactose/*N*-acetylglucosamine (detected as glucosamine)/glucose of 2.4:1.56:1.2 (expected monosaccharide ratios for reduced SGNL-oligosaccharides (60% $SGNL_4$/40% $SGNL_6$) = 2.4:1.4:1). Based on the galactose recovery from the SGNL-BSA derivative, an average of 7.5 SGNL-oligosaccharides were attached per BSA molecule. In addition, laser desorption mass spectroscopy was performed on the parent BSA and the SGNL-BSA conjugate. The parent BSA spectrum exhibited a peak of molecular ions centered at 68,400 mass units, while the SGNL-BSA derivative spectrum exhibited a broader peak of molecular ions centered at 75,000 mass units (data not shown). The difference, 6,600 mass units, is equivalent to a derivatization ratio of 6 SGNL-oligosaccharides attached per BSA molecule. The covalent attachment of intact SGNL-oligosaccharides to BSA was confirmed by SDS-PAGE of radioiodinated SGNL-BSA and Western blot analysis with HNK-1 antibody, which requires the presence of the sulfate on the SGNL-lipid for recognition

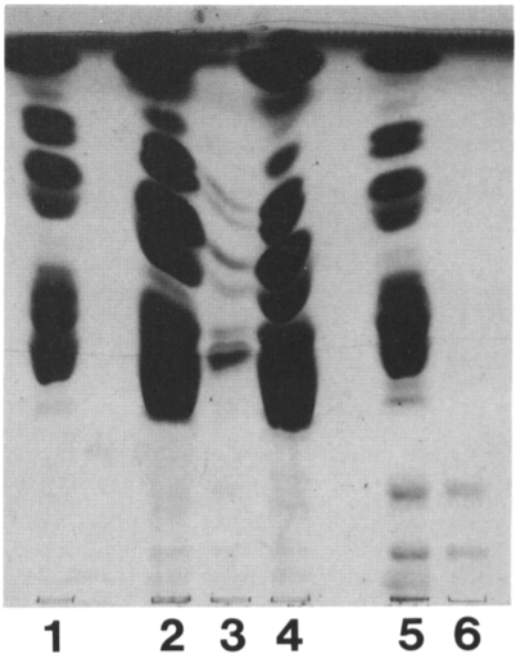

Figure 1. TLC analysis of SGNL-lipid purification from dog sciatic nerve endoneurium. Aliquots of lipid fractions derived from dog sciatic endoneurium were applied to high performance TLC plates, developed in chloroform/methanol/0.25% aqueous KCl (60:35:8), and visualized by $CuSO_4$/phosphoric acid char (61). Lipids were applied in amounts relative to the indicated starting wet weight of tissue: 1 mg (lane *1*) and 2.5 mg (lane *2*) equivalents of total lipid extract; 2.5 mg (lane *3*) and 50 mg (lane *5*) equivalents of the insoluble lipid residue resulting from reextraction of total lipids with chloroform/methanol (1:1); 2.5 mg equivalents (lane *4*) of the lipids soluble in the chloroform/methanol (1:1) reextraction; and 50 mg equivalents (lane *6*) of the purified SGNL-lipid fraction derived from further fractionation of the chloroform/methanol (1:1) insoluble residue as detailed in Materials and Methods.

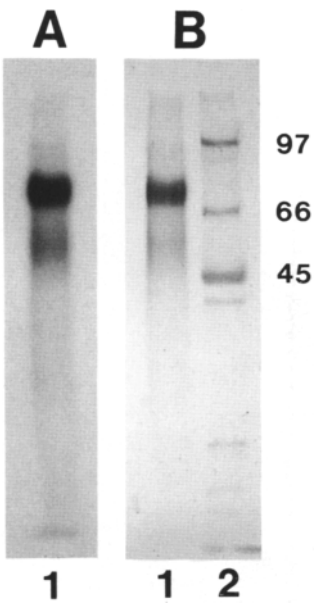

Figure 2. Immunoblot and autoradiographic analysis of ^{125}I-SGNL-BSA. Samples of ^{125}I-SGNL-BSA (lane *1*) and biotinylated molecular weight markers (lane 2) were subjected to electrophoresis in a 10–20% SDS-polyacrylamide gel under reducing conditions and transferred to nitrocellulose for fluorographic (*A*) and immunoblot (*B*) analysis. The immunoblot was incubated with HNK-1 antibody and bound antibody was detected with biotinylated goat anti-mouse IgM followed by avidin/biotinylated horseradish peroxidase complex. Molecular masses of the biotinylated molecular mass markers (in kD), including BSA (66 kD) are indicated.

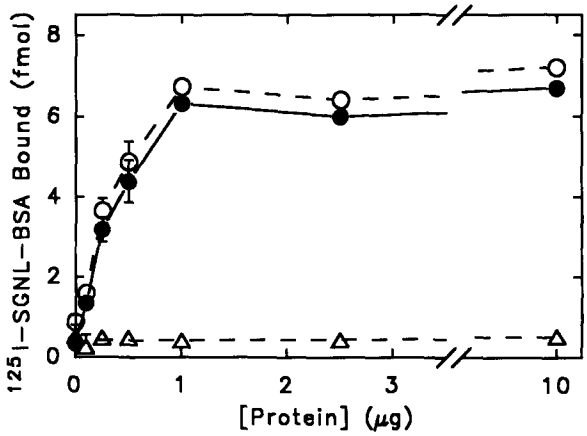

Figure 3. Calcium-dependent binding of ^{125}I-SGNL-BSA to rat PNS myelin as a function of membrane protein concentration. The indicated amounts of rat PNS myelin-enriched membranes (fraction S1A, see Materials and Methods) were incubated with 0.7 nM ^{125}I-SGNL-BSA for 30 min at 4°C in a total volume of 250 μl binding buffer in the presence or absence of 20 mM $CaCl_2$, and membrane-bound ligand was separated from free ligand by filtration. Nonspecific binding in the absence of calcium (△) was subtracted from total binding in the presence of calcium (○) to yield specific binding (●). Values are the mean ± SD for triplicate (total) or duplicate (nonspecific) determinations (SD values which fall within the symbols are not shown).

(24). The radioiodinated conjugate migrated as a broad band, with a major radioiodinated product comigrating with the HNK-1 reactive band at an apparent molecular weight greater than that of BSA (Fig. 2). No HNK-1 binding was detected against underivatized BSA (data not shown). The derivative is denoted $(SGNL)_7BSA$, or simply SGNL-BSA, to be consistent with prior neoglycoconjugate terminology (28).

^{125}I-SGNL-BSA Binding to Rat Peripheral Nerve Myelin Membranes

Rat PNS myelin-enriched membranes were isolated by differential centrifugation and discontinuous sucrose gradient fractionation of rat sciatic nerve endoneurium. When ^{125}I-SGNL-BSA (0.7 nM) was incubated with increasing amounts of rat PNS myelin-enriched membranes and the bound ligand separated from the free ^{125}I-SGNL-BSA by filtration, membrane-dependent binding was readily detected. Background binding was very low, ~0.4% of the total added radioligand in the absence of added membranes. Initial experiments demonstrated that 10 μM SGNL-lipid reduced the binding of the ^{125}I-SGNL-BSA to the same low background levels, as did omitting calcium from the binding buffer (see below). In subsequent experiments, specific binding was defined as binding to membranes in the presence of 20 mM $CaCl_2$ (total) less binding in the absence of calcium or in the absence of membranes (nonspecific). Binding increased proportionally with added membranes up to 1 μg membrane protein (Fig. 3).

In the presence of 0.5 nM ^{125}I-SGNL-BSA, binding to rat PNS membranes reached equilibrium within 30 min at 4°C (Fig. 4, filled circles). This incubation time was chosen for subsequent binding studies. Binding as a function of the amount of membranes added indicated that the maximum amount of radioligand bound was well below that added (see Fig. 3). This was not unexpected, since the synthetic multivalent ligand is inherently heterogeneous (see below). To determine if the ^{125}I-SGNL-BSA which remained unbound was competent to bind to fresh membranes, membrane-bound radioligand was separated from free radioligand by filtration and a second aliquot of membranes was added to the free ^{125}I-SGNL-BSA in the filtrate. Radioligand bound after a second incubation of 30 min was then determined (Fig. 4, open circles). The sum of the ^{125}I-SGNL-BSA bound after the first and second incubations, expressed as a percent of the input ligand, was constant and indicated that ~6% of the ^{125}I-SGNL-BSA was competent to bind to rat PNS myelin-enriched membranes (Fig. 4, triangles). Inclusion of the protease inhibitors phenylmethylsulfonylfluoride, leupeptin, antipain, benzamidine, aprotinin, chymostatin, and pepstatin in the binding buffer did not affect the kinetics of binding nor the maximal amount of radioligand bound (data not shown). To evaluate the molecular heterogeneity of the bound and the free ^{125}I-SGNL-BSA, membrane-bound radioligand was separated from free radioligand by centrifugation, and the two pools were analyzed by Western blot HNK-1 immunostaining and autoradiography subsequent to SDS-PAGE. Both pools were HNK-1 reactive: the free ^{125}I-SGNL-BSA was indistinguishable from the total ^{125}I-SGNL-BSA, while the bound ^{125}I-SGNL-BSA exhibited enrichment for higher molecular weight HNK-1 reactive iodinated species. (No HNK-1 staining was detected against rat PNS membranes alone, data not shown.)

Binding isotherms were performed with increasing concentrations of ^{125}I-SGNL-BSA incubated for 30 min with 0.25 μg membrane protein. As the concentration of ^{125}I-SGNL-BSA was increased, nonspecific background binding of radioligand (binding to filters in the absence of membranes but presence of calcium [Fig. 5 *A*, triangles], or in the presence of membranes but absence of calcium [not shown]) increased in a nonsaturable, linear manner as expected. Specific binding of ^{125}I-SGNL-BSA to rat PNS myelin-enriched membranes was saturable and exhibited high

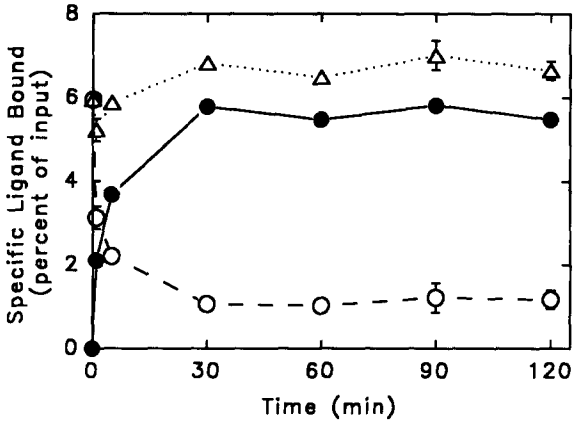

Figure 4. Kinetics of ^{125}I-SGNL-BSA binding to rat PNS myelin and competency of the unbound radioligand to bind fresh membranes. Rat PNS myelin-enriched membranes (fraction S1A) were incubated with 0.5 nM ^{125}I-SGNL-BSA under standard conditions except that the volume of each binding reaction was increased 8-fold to 2 ml and the total membrane protein added to each reaction was 60 μg. After the indicated times at 4°C, the reaction was filtered through glass fiber filters (Whatman GFC) and the filtrate collected for further use (see below). The filters were then rapidly washed, collected, and radioactivity quantitated to determine binding kinetics (●). To 225 μl of the binding assay filtrate collected at each indicated time was added fresh myelin membranes (7.5 μg in 25 μl 0.29 M sucrose). After an additional 30 min at 4°C, ligand bound to membranes after this second incubation was separated from free ligand by filtration and quantitated as in the standard assay to determine the percent of unbound ligand at each time which was competent to bind to fresh membranes (○). Nonspecific binding (in the absence of $CaCl_2$, < 0.8% of added ligand) was determined in parallel incubations and was subtracted from total binding. Data are presented as percent of added ligand specifically bound during the initial incubation (●), after the second incubation with fresh membranes (○) and the sum of these two incubations (△). Values are the mean ± SD for triplicate determinations (SD values which fall within the symbols are not shown).

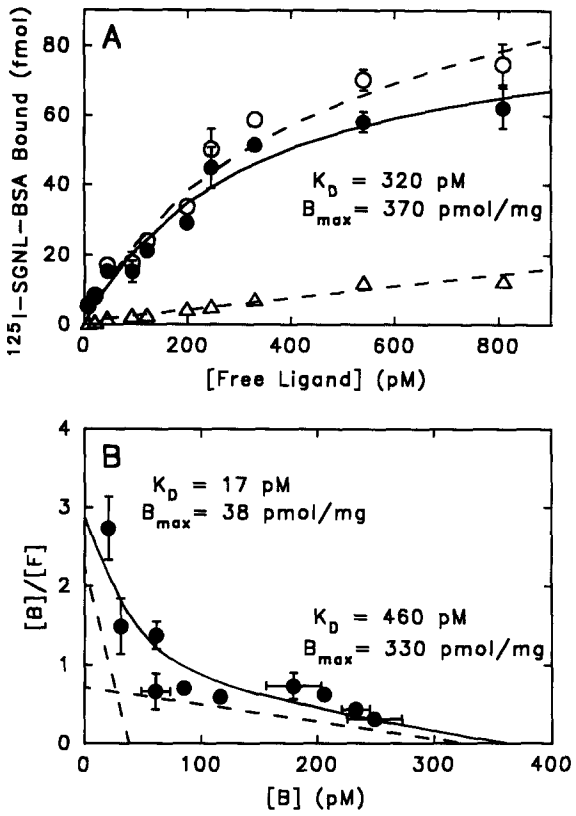

Figure 5. Saturation isotherms for ^{125}I-SGNL-BSA binding to rat PNS myelin. (*A*) Rat PNS myelin-enriched membranes (fraction S1A, 0.25 μg protein) were incubated with increasing concentrations of ^{125}I-SGNL-BSA in 250 μl binding buffer containing 20 mM $CaCl_2$. After 30 min at 4°C, membrane-bound ligand was separated from free ligand by filtration (○, total ligand bound). Nonspecific ligand bound (△) was determined in parallel incubations in the absence of membranes, and was subtracted from total bound to calculate specific bound (●). Values are the mean ± SD for quadruplicate (total binding) or triplicate (nonspecific binding) determinations (SD values that fall within the symbols are not shown). The abscissa is the concentration of free ^{125}I-SGNL-BSA competent to bind PNS myelin membranes (see text). Free ligand was calculated as the amount of radioligand added times the proportion of ligand (5.3%) competent to bind (to an excess of membranes, 10 μg) less the specifically bound ligand. The solid line was generated by a nonlinear fit of the specific binding data using a single site binding model and yielded the indicated apparent dissociation constant (K_D) and total receptor density (B_{max}). (*B*) Scatchard transformation of specific ^{125}I-SGNL-BSA binding to rat PNS myelin. Data for the specific binding isotherm (Fig. 5 *A*) was transformed by the method of Scatchard (49) (●). The dashed lines were fit to the curve using a two-site model and yielded the indicated apparent dissociation constant (K_D) and total receptor concentration (B_{max}) values.

affinity (Fig. 5 *A*, filled circles). Nonlinear fit of the data using a single site model resulted in a K_D of 320 pM and a B_{max} of 370 pmol/mg protein (Fig. 5 *A*, solid line). However, unexpectedly high binding at the lower end of the titration curve was consistently observed, and Scatchard transformation (49) of the binding isotherm data was curvelinear (Fig. 5 *B*), consistent with the presence of a low abundance, higher-affinity subpopulation of binding sites when fit to a two site model (high-affinity class K_D = 17 pM, B_{max} = 38 pmol/mg membrane protein; lower-affinity class K_D = 460 pM, B_{max} = 330 pmol/mg membrane protein). For determining binding constants, the unbound (free) ligand concentration was calculated based on the proportion of total ^{125}I-SGNL-BSA competent to bind rat PNS myelin-enriched membranes (see Fig. 4), which was experimentally determined in a parallel binding assay containing 0.5 nM ligand and an excess (10 μg) of membrane protein.

Experiments to test whether SGNL-specific antibodies (23) would block ^{125}I-SGNL-BSA binding to membranes were inconclusive, since control immunoglobulins (mouse IgM and IgG) interfered with the binding assay as did the corresponding monoclonals HNK-1 (IgM) and F7F7 (IgG) (data not shown). The basis of the interference was not determined.

Divalent Cation, Ionic Strength, and pH Effects on ^{125}I-SGNL-BSA Binding

Ligand binding was studied as a function of divalent cation concentration, using a variety of divalent cations over a broad concentration range (Table I). Divalent cations were required for binding and calcium supported higher specific binding than other divalent cations tested. Half-maximal binding of ^{125}I-SGNL-BSA to rat PNS myelin occurred at 5 mM Ca^{+2}, with maximal binding at 10 mM Ca^{+2} (Fig. 6).

Table I. Effects of Divalent Cations on ^{125}I-SGNL-BSA Binding to PNS Myelin

Divalent ion	Concentration	^{125}I-SGNL-BSA Bound*
	mM	*% of control*
None		0.1 ± 0.3
$SrCl_2$	2.5	7.9 ± 3.9
	5	25 ± 3.3
	10	51 ± 6.9
	20	88 ± 9.4
	30	62 ± 3.2
	40	45 ± 3.9
$MgCl_2$	2.5	11 ± 9.8
	10	21 ± 6.8
	20	38 ± 2.8
	30	35 ± 3.2
$BaCl_2$	2.5	7.4 ± 1.0
	10	27 ± 3.0
	20	34 ± 4.5
	30	21 ± 1.9
$CoCl_2$	2.5	9.4 ± 4.5
	10	27 ± 3.0
	20	33 ± 2.9
	30	20 ± 2.7
$MnCl_2$	2.5	4.4 ± 2.2
	10	10 ± 3.8
	20	26 ± 10
	30	35 ± 4.4
	40	52 ± 2.7

Rat PNS myelin-enriched membranes (fraction S1A, 0.25 μg protein) were incubated with 0.5 nM ^{125}I-SGNL-BSA for 30 min at 4°C in 250 μl binding buffer containing the indicated divalent cation salts in the absence of $CaCl_2$. Values are the mean ± SD for triplicate determinations.
* Specific binding was determined at each salt concentration by subtracting nonspecific binding in the absence of membranes from total binding in the complete reaction. Data are expressed as the percent of control specific binding in the presence of 20 mM $CaCl_2$ (specific binding for three experiments ranged from 2.5 to 5.8 fmol per reaction).

Among other divalent cations tested, Sr^{+2} supported maximal binding that was 88% of that in the presence of Ca^{+2}, while other divalent cations (Ma^{+2}, Ba^{+2}, Co^{+2}, and Mn^{+2}) supported much less binding (Table I). While divalent cations were required for binding, they could be omitted from the filter wash buffer without reducing specific binding, suggesting that little dissociation occurred during the rapid (~1 min) wash. Subsequent experiments were performed with divalent cation omitted from the filter wash.

Increasing ionic strength decreased specific binding, as can be seen with higher calcium chloride concentrations (Fig. 6). Similarly, addition of $MgCl_2$, $MgSO_4$, NaCl, or KCl reduced radioligand binding to half-maximal levels at concentrations ranging from ~25 to 50 mM. No significant variation in binding was detected over the pH range of 6.0–8.0 (in 50 mM imidazole acetate buffer).

Subcellular and Nervous System Distribution of ^{125}I-SGNL-BSA Binding

Peripheral nerve membrane fractions were isolated by differential centrifugation and discontinuous sucrose gradient centrifugation. Sciatic nerve endoneurium homogenate was centrifuged (low speed) to yield a crude supernatant fraction (S1), a portion of which was centrifuged at higher speed to yield a mixed membrane (P2) fraction. Most of the

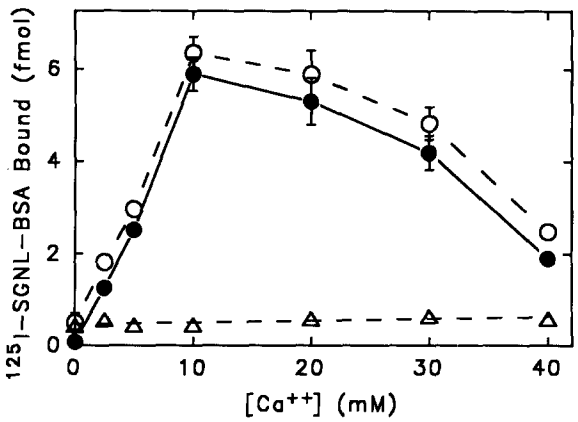

Figure 6. Binding of ^{125}I-SGNL-BSA to rat PNS myelin as a function of calcium concentration. Rat PNS myelin-enriched membranes (fraction S1A, 0.25 μg protein) were incubated with 0.5 nM ^{125}I-SGNL-BSA for 30 min at 4°C in a total volume of 250 μl binding buffer containing the indicated concentrations of $CaCl_2$, and the membrane-bound ligand was separated from the free ligand by filtration (○, total binding). Nonspecific binding (△) was determined in parallel incubations in the absence of membranes, and was subtracted from total binding to calculate specific binding (●). Values are the mean ± SD for triplicate (total binding) or duplicate (nonspecific binding) determinations (SD values that fall within the symbols are not shown).

crude S1 was subjected to discontinuous sucrose gradient centrifugation to yield myelin-enriched membranes (S1A) and denser mixed membranes (S1B). A portion of S1A was further subjected to osmotic shock and a second discontinuous sucrose gradient, to generate myelin fraction S2 (42). ^{125}I-SGNL-BSA binding was clearly enriched in fractions containing PNS myelin (Fig. 7 *A*, Table II), while denser PNS membranes (S1B) had little binding activity.

Membrane fractions were also prepared from the CNS for comparison to PNS myelin binding of ^{125}I-SGNL-BSA. A mixed membrane P2 fraction prepared from whole rat brain by differential centrifugation (11) and consisting of myelin membranes, synaptosomes, and mitochondria, had very low binding activity (Fig. 7 *B*), as did brain membranes further fractionated by discontinuous sucrose density centrifugation to yield crude myelin (P2A) and crude synaptosomal (P2B) fractions (19). Under identical conditions, PNS myelin membranes bound 20–40-fold more ^{125}I-SGNL-BSA than did any of the CNS membrane fractions.

Among adult CNS brain regions, SGNL-lipids are found exclusively in the cerebellum (43). Therefore, cerebellar P2 membranes were prepared and tested for ^{125}I-SGNL-BSA binding activity. Like whole brain membrane fractions, cerebellar membranes failed to bind significant ligand (Fig. 7 *B*).

Carbohydrate Specificity of ^{125}I-SGNL-BSA Binding

Various compounds including SGNL-lipids and other sulfolipids, gangliosides, neutral glycosphingolipids, phospholipids, mono- and oligosaccharides, glycosaminoglycans, and other anionic polysaccharides, were tested for their ability to inhibit ^{125}I-SGNL-BSA binding to rat PNS myelin-enriched membranes.

SGNL-lipids isolated from two sources, human and bovine cauda equina, were the most potent of the lipids tested

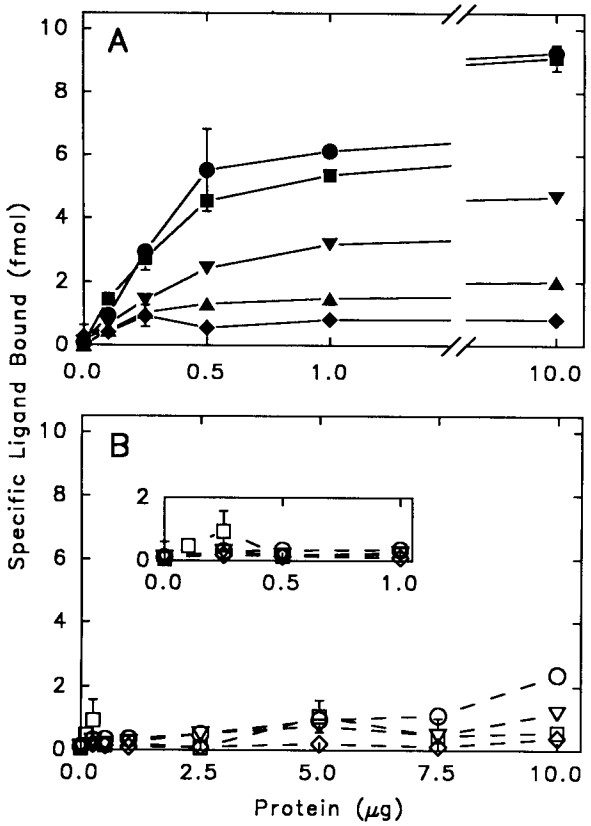

Figure 7. Binding of ^{125}I-SGNL-BSA to rat PNS endoneurium and brain subcellular fractions. (*A*) Rat peripheral nerve endoneurium homogenate was fractionated by differential centrifugation (▲, crude homogenate, S1; ▼, mixed membranes, P2) and discontinuous sucrose gradient centrifugation of S1 (●, myelin-enriched, S1A; ♦, dense-membranes, S1B), or of osmotically shocked S1A (■, S2) as described in Materials and Methods. (*B*) Whole rat brain homogenate was fractionated by differential centrifugation (▽, mixed membranes, P2) and discontinuous sucrose gradient centrifugation (○, myelin-enriched, P2A; ◇, synaptosomes, P2B), and rat cerebellum homogenate was fractionated by differential centrifugation (□, mixed membranes, cerebellar, P2) as described in Materials and Methods. Specific binding of 0.5 nM ^{125}I-SGNL-BSA to aliquots of PNS or CNS fractions containing the indicated amounts of protein was determined as described in Fig. 3. Values are the mean ± SD for triplicate determinations (SD values which fall within the symbols are not shown).

as inhibitors (Fig. 8, Table III), with IC_{50} values in the submicromolar range. Gangliosides (sialic acid–bearing anionic glycosphingolipids) exhibited a range of inhibitory potencies, all less potent than SGNL-lipid. The gangliosides G_{M1} and G_{D1b} failed to inhibit half-maximally even when present at 100 μM, while G_{T1b} and G_{D1a} inhibited binding with average IC_{50}'s of ≥33 μM. Unlike inhibition by SGNL-lipids, there was significant variability in ganglioside inhibition between experiments (Table III). Gangliosides with neutral saccharide core structures of the neolacto series (the same neutral core as SGNL-lipids) were also tested as inhibitors: sialylneolactotetraosylceramide (41% sialyl[2–3], 59% sialyl[2–6]) inhibited with an IC_{50} of 40 μM, while the sialylated fucosylated neolactotetraosylceramides 2,3 sialyl Lewis x- and 2,6 sialyl Lewis x glycolipids failed to inhibit significantly at 10 μM (the highest concentration tested).

Table II. ^{125}I-SGNL-BSA Binding Activity to Peripheral Nerve Membrane Fractions

Fraction	Total protein	Binding activity	Binding recovery	Binding enrichment
	mg	*pmol/mg protein*	*%*	*-fold*
S1	42.8	3.8 ± 1.0	100	1.0
P2	23.8	5.8 ± 1.0	85	1.5
S1A	17.7	10.7 ± 1.2	116	2.8
S1B	0.8	3.0 ± 1.7	1.5	0.8
S2	6.8	11.5 ± 2.8	48	3.0

Specific binding of ^{125}I-SGNL-BSA to peripheral nerve homogenate (S1), crude membranes (P2), and fractions prepared by successive discontinuous sucrose gradient centrifugation (S1A, S1B, and S2) as detailed in Materials and Methods was determined as described in the legend to Fig. 3. The specific binding activity is reported as the mean ± SD for three determinations performed in triplicate in the linear protein range (0.1, 0.25, and 0.5 μg membrane protein, see Fig. 7).

The sulfated lipids sulfatide and cholesterol sulfate inhibited with moderate potency (IC_{50}'s ≥8 μM).

Neutral glycosphingolipids and most phospholipids failed to inhibit half-maximally even at 100 μM. Phosphatidylglycerol did inhibit, although its inhibition was dependent upon the fatty acid content. Synthetic phosphatidylglycerol having fully saturated fatty acids was noninhibitory (at 100 μM), while phosphatidylglycerol having saturated fatty acids inhibited with an IC_{50} of 8.3 μM. The significance of this observation is unknown.

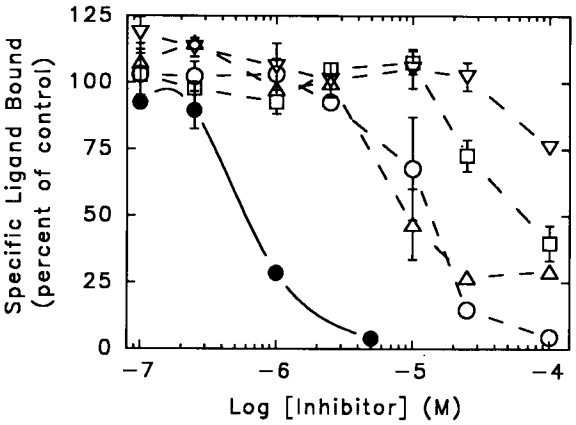

Figure 8. Inhibition of ^{125}I-SGNL-BSA binding to rat PNS myelin by lipids. Rat PNS myelin-enriched membranes (fraction S1A, 7.5 μg protein) were preincubated with the indicated concentrations of inhibitor for 30 min at 4°C in 225 μl binding buffer in the presence or absence of $CaCl_2$, and then ^{125}I-SGNL-BSA was added to a final concentration of 0.5 nM (250 μl total binding buffer volume). After further incubation for 30 min at 4°C, membrane-bound ligand was separated from free ligand by filtration. At each inhibitor concentration, the amount of ^{125}I-SGNL-BSA specifically bound (defined as binding to membranes in the presence of 20 mM $CaCl_2$ minus nonspecific binding to membranes in the absence of $CaCl_2$) was determined and is expressed as the percent of specific control binding in the absence of inhibitor (control binding was 5.8 ± 0.1 fmol). Values are the mean ± SD for triplicate determinations (SD values which fall within the symbols are not shown). The lipids tested were ●, SGNL-lipid (human); △, sulfatide; ○, cholesterol sulfate; □, G_{T1b}; and ▽, G_{D1a}. Non-inhibitory lipids (not shown) are listed in Table III.

Table III. Inhibition of ^{125}I-SGNL-BSA Binding to PNS Myelin by Lipids

Lipids (n)	IC_{50} (range)
	μM
SGNL-lipid, bovine (5)	0.99 (0.55–1.2)
SGNL-lipid, human (7)	0.48 (0.3–0.6)
Desulfated SGNL-lipid, human (2)	1.5 (1–2)
Methyl esterified, desulfated SGNL-lipid, human (1)	>25
sulfatide (4)	8.2 (4–12)
cholesterol sulfate (2)	10 (6.2–14)
sialylneolactotetraosylceramide (1)	40
2,3 sialyl Lewis x glycolipid (1)	>10
2,6 sialyl Lewis x glycolipid (1)	>10
G_{T1b} (4)	33 (6–64)
G_{D1a} (2)	58 (15–>100)
G_{D1b} (2)	>100
G_{M1} (1)	>100
globotetraosylceramide (1)	>100
galactosylceramide (1)	>100
phosphatidylglycerol (2)*	>100
phosphatidylinositol (1)	>100
phosphatidylinositolbisphosphate (1)	>100
phosphatidylserine (1)	>100
phosphatidic acid (1)	>100
phosphatidylcholine (1)	>100
phosphatidylethanolamine (1)	>100

Inhibition studies were performed as described in the legend to Fig. 8. The mean and range of concentrations of each inhibitor resulting in 50% inhibition (IC_{50}) of specific ^{125}I-SGNL-BSA binding in the absence of inhibitor was determined graphically from the indicated number (n) of independent binding experiments performed at four to seven concentrations of each inhibitor in triplicate. Control binding was comparable to that shown in Fig. 3.
* Results are for phosphatidylglycerol having unsaturated fatty acid chains ($C_{18:0}$). The same phospholipid having a mixture of natural fatty acids had an IC_{50} of 8.3 μM. Other phospholipids tested had natural fatty acids.

The molecular determinants responsible for inhibition of ^{125}I-SGNL-BSA binding to rat PNS myelin were investigated using chemically modified SGNL-lipid. Treatment of the SGNL-lipid with methanolic HCl resulted in concomitant removal of the 3-*O*-sulfate from the nonreducing terminal glucuronic acid and methyl esterification of the carboxylic acid at the 6-position of the glucuronic acid (6). A portion of the methyl esterified glycolipid was converted to the desulfated parent molecule by alkali treatment (6). Desulfated SGNL-lipid remained one third as potent as the parent SGNL-lipid in inhibiting ^{125}I-SGNL-BSA binding to rat PNS myelin. In contrast, methyl esterification of the desulfated SGNL-lipid blocked its ability to inhibit (Fig. 9, Table III).

Anionic monosaccharides (glucuronic acid and *N*-acetylneuraminic acid), SGNL oligosaccharides (liberated from dog SGNL-lipids by ceramide glycanase), and 3′-sialyllactose did not inhibit ^{125}I-SGNL-BSA binding to rat PNS myelin membranes at the highest concentrations tested (5 mM). Glycosaminoglycans (polysaccharides containing uronic acids and/or sulfated saccharide residues), and dextran sulfate (a synthetic sulfated polysaccharide) inhibited binding without specificity when added in the range of 0.1 μg/ml. Colominic acid, an anionic polymer of sialic acids, was a weaker inhibitor, with an IC_{50} of 100 μg/ml.

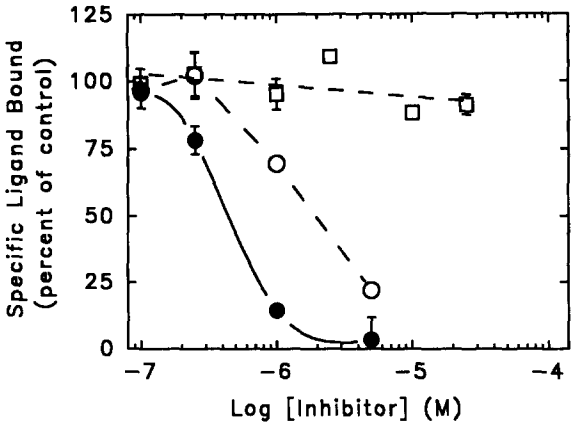

Figure 9. Inhibition of ^{125}I-SGNL-BSA binding to rat PNS myelin by SGNL-lipid derivatives. Desulfated and methyl esterified SGNL-lipid (□) and desulfated SGNL-lipid (○) were prepared from human SGNL-lipid (●) as described in Materials and Methods. Inhibition studies were performed as described in Fig. 8. ^{125}I-SGNL-BSA specifically bound at each lipid concentration is expressed as the percent of specific control binding in the absence of inhibitor (control binding was 5.2 ± 0.3 fmol). Values are the mean ± SD for triplicate determinations (SD values which fall within the symbols are not shown).

Protease Sensitivity of ^{125}I-SGNL-BSA Binding Activity

Preincubation of 0.25 μg of PNS myelin membrane protein with 0.01–0.5 μg trypsin and subsequent inactivation of the trypsin through the addition of soybean trypsin inhibitor resulted in a concentration dependent attenuation of ^{125}I-SGNL-BSA binding to <50% of control. Increasing trypsin to 5 μg during the preincubation (with subsequent addition of trypsin inhibitor) did not result in a further decrease in radioligand bound, which remained at 29–51% of that bound to control membranes in various experiments. Pretreatment of membranes with trypsin inhibitor alone or with trypsin in the presence of trypsin inhibitor had little effect on the amount of radioligand bound (data not shown). Pronase pretreatment of myelin membranes (12.5 μg of membrane protein pretreated with 0.01–5 μg pronase, and the membranes recovered by centrifugation in the presence of excess BSA) also resulted in a concentration dependent, but incomplete, reduction of ^{125}I-SGNL-BSA binding to 42% of that bound to control membranes. Binding activity on myelin membranes was heat stable, in that boiling did not reduce the amount of radioligand bound.

Discussion

The formation and maintenance of the multilamellar myelin sheath of axons depend upon coordinate cell surface recognition and interaction, both between the apposed membranes of the myelin-forming cell and the neuron, and between the scrolled myelin membranes themselves. Several coexisting families of adhesion molecules involving direct protein to protein interaction have been implicated in these cell–surface interactions of the myelin-forming cell of the PNS, the Schwann cell. We have focused on the potential role of carbohydrates as determinants recognized by Schwann cell surface receptors, and have proposed that the unusual sulfoglucuronylneolacto-glycolipids may function as recognition

ligands involved in myelination or myelin maintenance. Consistent with this role, our previous studies demonstrated that SGNL-lipids specifically support Schwann cell adhesion.

Our strategy to identify the hypothetical SGNL receptor on PNS myelin depended on the synthesis of a complementary high affinity radioligand. Since carbohydrate recognition often requires appropriate juxtaposition of multiple carbohydrate binding determinants (32), we constructed a multivalent SGNL-derivatized ligand that could be readily radiolabeled. This task was facilitated by a relatively rapid purification technique for SGNL-lipids and by the use of the enzyme ceramide glycanase to release SGNL-oligosaccharides, which could be linked to a BSA carrier to generate a multivalent radioiodinated ligand, ^{125}I-SGNL-BSA. Carbohydrate analysis confirmed the multivalent nature of the ligand, and immunoblot analysis subsequent to SDS-PAGE indicated that HNK-1 reactive epitopes were covalently attached to the BSA. Since HNK-1 reactivity requires the sulfate on the glucuronyl moiety and is abrogated if the glucuronyl carboxyl moiety is removed (24), the immunoblot data demonstrated that $(SGNL)_7$BSA carried intact sulfoglucuronyl epitopes.

^{125}I-SGNL-BSA was a successful ligand for identifying SGNL-directed binding activity on PNS membranes. The characteristics of this high-affinity and saturable binding activity were remarkable for a number of reasons. Within the PNS, binding was enriched on myelin rather than denser membranes. This suggests that the binding activity is a product of Schwann cells, and may be involved in their myelinating function. Our previous finding that intact primary Schwann cells bind to SGNL-lipids resolved by TLC chromatograms (38, 39) is consistent with a cell adhesion function for SGNL lipids and complementary Schwann cell receptors. The absence of ^{125}I-SGNL-BSA binding on CNS membranes, and especially on CNS myelin, is also of note. A CNS myelin ganglioside binding activity which appears to be a product of oligodendrocytes, but which is absent from PNS myelin, may be a complementary CNS system for axon recognition (58, 59).

The possibility that the SGNL-binding site is a membrane protein is supported by the finding that preincubation of PNS myelin membranes with trypsin or pronase partially abrogates the subsequent binding of ^{125}I-SGNL-BSA to these membranes. The observation that binding of ^{125}I-SGNL-BSA was calcium-dependent may relate this activity to a family of vertebrate calcium–dependent carbohydrate binding proteins (15) including the selectins (54) and the glycoprotein receptors on hepatocytes and macrophages. The calcium requirement clearly distinguishes this activity from the broadly distributed galactose binding proteins which can be found in the PNS (21) as well as from the CNS myelin ganglioside binding activity mentioned above (59).

A consistent observation during these studies was that only a small portion of added radioligand (~6%) specifically bound to PNS myelin membranes, even when membranes were added in excess. The observations that recovered, unbound ^{125}I-SGNL-BSA did not bind to fresh membranes, yet remained as macromolecular, HNK-1 reactive material, suggests that the ligand itself is structurally heterogeneous. This is not surprising, since random glycosylation of an average of 7.5 of the 60 lysines on BSA would be expected to generate a statistical variation in glycosylation number and even more variation in the relative spatial arrangement of oligosaccharides on the carrier. Studies in other carbohydrate recognition systems demonstrate that precise spatial relationships can be critical to high-affinity binding of multivalent glycoconjugates (32, 46). Our data suggest that the valence and/or the spatial arrangement of the oligosaccharides on a subpopulation (~6%) of the ^{125}I-SGNL-BSA molecules is appropriate for high-affinity ligand binding. SGNL-lipids in natural membranes are most likely laterally mobile and may adopt the required valence and juxtaposition. Consistent with this model, monovalent SGNL-oligosaccharides failed to inhibit binding of the multivalent derivative to PNS myelin even when present at concentrations as high as 5 mM. In contrast, SGNL-lipids, added as detergent mixed micelles, specifically inhibited binding with an $IC_{50} < 1$ μM. Such marked differences between glycolipids and their monovalent oligosaccharide constituents have also been reported for other carbohydrate recognition systems (32, 58).

In performing kinetic analyses of ^{125}I-SGNL-BSA binding, the maximum percentage of ligand competent to bind was experimentally determined to allow accurate calculation of the unbound, competent ligand concentration. Based on this analysis, the affinity is very high, with a K_D of 320 pM when fit to one site. However, Scatchard transformation of the binding isotherm was curvilinear, consistent with multiple classes of binding sites or ligands. The presence of multiple ligands with distinct binding affinities would be most consistent with our hypothesis that valence and spatial configuration of the SGNL-oligosaccharides on the carrier protein influence binding, although multiple classes of binding sites are also possible.

The higher binding affinity of the competent binding fraction of SGNL-BSA (K_D = 320 pM) compared to SGNL-lipid (K_I ~1 μM) may reflect differences in effective valence and/or presentation of the SGNL-oligosaccharides. Lipid inhibitors were added in the presence of 0.032% Triton X-100, a concentration sufficient to form micelles in which the lipids distribute, most likely at low valence. The orientation of the oligosaccharide chain may also be effected by glycolipid insertion in a detergent micelle. Nevertheless, the carbohydrate-specificity of ^{125}I-SGNL-BSA binding was notable, in that among many anionic and neutral glycosphingolipids and phospholipids tested under identical conditions, SGNL-lipid itself was the most potent inhibitor of ^{125}I-SGNL-BSA binding to PNS myelin (Table III). Surprisingly, the sulfate group on the glucuronic acid moiety was not required for SGNL-lipid recognition, although sulfate removal reduced SGNL-lipid inhibitory potency to one third that of the parent molecule. In contrast, esterification of the glucuronic acid (on desulfated SGNL-lipid) essentially eliminated its inhibitory activity (see Fig. 9). This is of interest, since nonsulfated forms of the SGNL-lipid are broadly distributed phylogenetically (14) and may be more ancient in evolution. Some role for the sulfate in binding was indicated by the observation that sulfatide (sulfate-3-galactosylceramide) inhibited ^{125}I-SGNL-BSA binding (with an order of magnitude lower potency than SGNL-lipid) while its parent molecule, galactosylceramide, failed to inhibit. Gangliosides, anionic glycosphingo-lipids containing carboxylic acid groups on sialic acid moieties rather than on glucuronic acid, were either noninhibitory or were much less potent inhibitors than SGNL-lipid or desulfated SGNL-lipid (Table III). Of par-

ticular note is that sialylneolactotetraosylceramide, which has the same neutral saccharide core as SGNL-lipid but with a sialic acid rather than a glucuronic acid linked to the 3-position of the outermost galactose, exhibited an inhibitory potency that was <4% that of the desulfated SGNL-lipid. Although the precise carbohydrate specificity has not been defined, these data suggest that the SGNL-binding site revealed by ^{125}I-SGNL-BSA binding has specificity for glucuronic acid moieties, and is enhanced by the sulfate group. This hypothesis is strengthened by the finding that glycosaminoglycans or polysulfated dextran inhibited the binding of ^{125}I-SGNL-BSA to PNS myelin much more potently than did colominic acid, an anionic polymer of sialic acid. These data indicate that charge density, per se, is not responsible for SGNL-BSA binding, although all highly multivalent sulfated or uronic acid–containing polymers tested were moderately potent inhibitors. For example, hyaluronic acid (glucuronic acid–*N*-acetylglucosamine copolymer) inhibited ^{125}I-SGNL-BSA binding at 0.1 μg/ml, or 260 nM in glucuronic acid residues. This can be compared to SGNL-BSA, which inhibited at 2.4 nM in glucuronic acid residues. Nevertheless, proteoglycan inhibition may indicate a meaningful specificity for this PNS-binding activity.

In some species, quantitatively minor isoforms of certain glycoproteins (including the PNS myelin adhesive glycoproteins MAG and P_0) bind to HNK-1 antibodies, raising the possibility that the SGNL-binding activity we have identified is directed towards these glycoproteins rather than glycolipids. This is particularly unlikely in the rat PNS, where MAG and P_0 do not carry HNK-1 reactive epitopes (41). Therefore, it is likely that the binding activity that we have characterized is functionally specific for interaction with SGNL glycosphingolipids. More direct tests of glycoprotein vs. glycolipid binding specificity experiments are not yet meaningful, since the SGNL structure has yet to be identified on any of the HNK-1-reactive glycoproteins.

Some well defined proteins have been previously reported to bind to SGNL-lipids, including laminin (36), P30 (37), serum amyloid P component (34), and L- and P-selectins (40). Of these, laminin is a component of Schwann cell basement membranes (10), and P30 has been found in Schwann cells and the peripheral nerve (13) while the selectins and amyloid P have not been reported in the peripheral myelin. The binding characteristics and tissue distribution differentiate these proteins from the novel binding activity detected in PNS myelin in this study. Neither laminin nor P30 exhibits calcium dependence for binding to SGNL-lipids. Furthermore, laminin has greater avidity for sulfatide than for SGNL-lipids and requires the sulfate on SGNL-lipids for avid binding (36). While the carbohydrate structural specificity of P30 has not been as fully established, it was isolated from rat cerebellar membranes (37) where we were unable to detect ^{125}I-SGNL-BSA binding. L- and P-selectins bind avidly to sialyl Lewis x glycolipids in a calcium-dependent manner, while their binding to SGNL-lipids is calcium-independent (40), both properties which are not shared by the PNS myelin ^{125}I-SGNL-BSA binding site.

In conclusion, we have identified and characterized a novel, calcium-dependent, tissue- and carbohydrate-specific SGNL-oligosaccharide–binding activity on rat PNS myelin. The prior observations (38, 39) that SGNL-lipids, which are present both in the axolemma and (in smaller amounts) in myelin and other Schwann cell membranes, support specific adhesion of rat Schwann cells suggest that the PNS myelin SGNL-lipid binding activity may be involved in Schwann cell–axon or myelin lamellae–lamellae membrane interactions necessary for myelination or myelin maintenance.

We thank Lynda Yang and Stephanie Edgar for valuable laboratory assistance; Drs. Robert Yu (Virginia Commonwealth University), Paul James and Brian Brandley (Glycomed, Inc.), and A. Hasegawa (Gifu University) for kind gifts of lipids; Dr. Richard Quarles (National Institutes of Health) for the generous gift of monoclonal antibody F7F7; Drs. Robert Cotter and Marc Chevrier for performing laser desorption mass spectroscopy analysis; and Dr. Hans Schweingruber for performing fast atom bombardment mass spectroscopy.

This work was supported in part by the National Institutes of Health grant HD14010 and the National Multiple Sclerosis Society grant RG2223. L. K. Needham was supported by training grant MH18030 from the National Institutes of Health.

Received for publication 3 November 1992 and in revised form 13 January 1993.

References

1. Ariga, T., T. Kohriyama, L. Freddo, N. Latov, M. Saito, K. Kon, S. Ando, M. Suzuki, M. E. Hemling, K. L. Rinehart, S. Kusunoki, and R. K. Yu. 1987. Characterization of sulfated glucuronic acid containing glycolipids reacting with IgM M-proteins in patients with neuropathy. *J. Biol. Chem.* 262:848–853.
2. Bounias, M. 1980. N-(1-napthyl)ethylenediamine dihydrochloride as a new reagent for nanomolar quantitation of sugars on thin-layer plates by a mathematical calibration process. *Anal. Biochem.* 106:291–295.
3. Brandley, B. K., S. J. Swiedler, and P. W. Robbins. 1990. Carbohydrate ligands of the LEC cell adhesion molecules. *Cell.* 63:861–863.
4. Cabacungan, J. C., A. I. Ahmed, and R. E. Feeney. 1982. Amine boranes as alternative reducing agents for reductive alkylation of proteins. *Anal. Biochem.* 124:272–278.
5. Chevrier, M. R., and R. J. Cotter. 1991. A matrix-assisted laser desorption time-of-flight mass spectrometer based on a 600 ps, 1.2 mJ nitrogen laser. *Rapid Commun. Mass Spectrom.* 5:611–617.
6. Chou, D. K. H., A. A. Ilyas, J. E. Evans, C. Costello, R. H. Quarles, and F. B. Jungalwala. 1986. Structure of sulfated glucuronyl glycolipids in the nervous system reacting with HNK-1 antibody and some IgM paraproteins in neuropathy. *J. Biol. Chem.* 261:11717–11725.
7. Chou, D. K. H., G. A. Schwarting, J. E. Evans, and F. B. Jungalwala. 1987. Sulfoglucuronyl-neolacto series of glycolipids in peripheral nerves reacting with HNK-1 antibody. *J. Neurochem.* 49:865–873.
8. Chou, D. K. H., N. Prasadarao, O. Koul, and F. B. Jungalwala. 1991. Developmental expression of HNK-1-reactive antigens in rat cerebal cortex and molecular heterogeneity of sulfoglucuronylneolactotetraosylceramide in CNS versus PNS. *J. Neurochem.* 57:852–859.
9. Cole, G. J., and M. Schachner. 1987. Localization of the L2 monoclonal antibody binding site on chicken neural cell adhesion molecule (NCAM) and evidence for its role in NCAM-mediated cell adhesion. *Neurosci. Lett.* 78:227–232.
10. Cornbrooks, C. J., D. J. Carey, J. A. McDonald, R. Timpl, and R. P. Bunge. 1983. In vivo and in vitro observations on laminin production by Schwann cells. *Proc. Natl. Acad. Sci. USA.* 80:3850–3854.
11. Cotman, C. W. 1974. Isolation of synaptosomal and synaptic plasma membrane fractions. *Methods Enzymol.* 31:445–452.
12. Dahms, N. M., and R. L. Schnaar. 1983. Ganglioside composition is regulated during differentiation in the neuroblastoma X glioma hybrid cell line NG108-15. *J. Neurosci.* 3:806–817.
13. Daston, M. M., and N. Ratner. 1991. Expression of P30, a protein with adhesive properties, in Schwann cells and neurons of the developing and regenerating peripheral nerve. *J. Cell Biol.* 112:1229–1239.
14. Dennis, R. D., H. Antonicek, H. Wiegandt, and M. Schachner. 1988. Detection of the L2/HNK-1 carbohydrate epitope on glycoproteins and acidic glycolipids of the insect *Calliphora vicina*. *J. Neurochem.* 51:1490–1496.
15. Drickamer, K. 1988. Two distinct classes of carbohydrate-recognition domains in animal lectins. *J. Biol. Chem.* 263:9557–9560.
16. Dulbecco, R., and M. Vogt. 1954. Plaque formation and isolation of pure lines with poliomyelitis viruses. *J. Exp. Med.* 99:167–182.
17. Feizi, T. 1991. Carbohydrate differentiation antigens: probable ligands for cell adhesion molecules. *Trends Biochem. Sci.* 16:84–86.
18. Fredman, P., O. Nilsson, J.-L. Tayot, and L. Svennerholm. 1980. Separation of gangliosides on a new type of anion-exchange resin. *Biochim. Biophys. Acta.* 618:42–52.

19. Gray, E. G., and V. P. Whittaker. 1962. The isolation of nerve endings from brain: an electron-microscopic study of cell fragments derived by homogenization and centrifugation. *J. Anat.* 96:79–88.
20. Handa, S., and Y. Kushi. 1984. Application of field desorption and secondary ion mass spectrometry for glycolipid analysis. *Adv. Exp. Med. Biol.* 174:65–73.
21. Hynes, M. A., L. B. Buck, M. Gitt, S. Barondes, J. Dodd, and T. M. Jessel. 1989. Carbohydrate recognition in neuronal development: structure and expression of surface oligosaccharides and β-galactoside-binding lectins. *Ciba Found. Symp.* 145:189–218.
22. Iida, N., T. Toida, Y. Kushi, S. Handa, P. Fredman, L. Svennerholm, and I. Ishizuka. 1989. A sulfated glucosylceramide from rat kidney. *J. Biol. Chem.* 264:5974–5980.
23. Ilyas, A. A., M. C. Dalakas, R. O. Brady, and R. H. Quarles. 1986. Sulfated glucuronyl glycolipids reacting with anti-myelin-associated glycoprotein monoclonal antibodies including IgM paraproteins in neuropathy: species distribution and partial characterization of epitopes. *Brain Res.* 385:1–9.
24. Ilyas, A. A., D. K. H. Chou, F. B. Jungalwala, C. Costello, and R. H. Quarles. 1990. Variability in the structural requirements for binding of human monoclonal anti-myelin-associated glycoprotein immunoglobulin M antibodies and HNK-1 to sphingoglycolipid antigens. *J. Neurochem.* 55:594–601.
25. Kameyama, A., H. Ishida, M. Kiso, and A. Hasegawa. 1991. Total synthesis of sialyl Lewis X. *Carbohydr. Res.* 209:c1–c4.
26. Keilhauer, G., A. Faissner, and M. Schachner. 1985. Differential inhibition of neurone-neurone, neurone-astrocyte, and astrocyte-astrocyte adhesion by L1, L2, and N-CAM antibodies. *Nature (Lond.).* 316: 728–730.
27. Kohriyama, T., S. Kusunoki, T. Ariga, J. E. Yoshino, G. H. DeVries, N. Latov, and R. K. Yu. 1987. Subcellular localization of sulfated glucuronic acid-containing glycolipids reacting with anti-myelin-associated glycoprotein antibody. *J. Neurochem.* 48:1516–1522.
28. Kuhlenschmidt, T. B., and Y. C. Lee. 1984. Specificity of chicken liver carbohydrate binding protein. *Biochemistry.* 23:3569–3575.
29. Künemund, V., F. B. Jungalwala, G. Fischer, D. K. H. Chou, G. Keilhauer, and M. Schachner. 1988. The L2/HNK-1 carbohydrate of neural cell adhesion molecules is involved in cell interactions. *J. Cell Biol.* 106:213–223.
30. Ladisch, S., and B. Gillard. 1985. A solvent partition method for microscale ganglioside purification. *Anal. Biochem.* 146:220–231.
31. Laemmli, U. K. 1970. Cleavage of structural proteins during the assembly of the head of bacteriophage T4. *Nature (Lond.).* 227:680–685.
32. Lee, Y. C. 1989. Binding modes of mammalian hepatic lectin Gal/GalNAc receptors. *Ciba Found. Symp.* 145:80–95.
33. Lee, Y. C. 1990. High-performance anion-exchange chromatography for carbohydrate analysis. *Anal. Biochem.* 189:151–162.
34. Loveless, R. W., G. Floyd-O'Sullivan, J. G. Raynes, C.-T. Yuen, and T. Feizi. 1992. Human serum amyloid P is a multispecific adhesive protein whose ligands include 6-phosphorylated mannose and the 3-sulphated saccharides galactose, N-acetylgalctosamine and glucuronic acid. *EMBO (Eur. Mol. Biol. Organ.) J.* 11:813–819.
35. Magnani, J. L., S. L. Spitalnik, and V. Ginsburg. 1987. Antibodies against cell surface carbohydrates: determination of antigen structure. *Methods Enzymol.* 138:195–207.
36. Mohan, P. S., D. K. H. Chou, and F. B. Jungalwala. 1990. Sulfoglucuronyl glycolipids bind laminin. *J. Neurochem.* 54:2024–2031.
37. Mohan, P. S., J. Laitinen, J. Merenmies, H. Rauvala, and F. B. Jungalwala. 1992. Sulfoglycolipids bind to the adhesive protein amphoterin (P30) in the nervous system. *Biochem. Biophys. Res. Commun.* 182: 689–696.
38. Needham, L. K., and R. L. Schnaar. 1990. Adhesion of primary Schwann cells to HNK-1 reactive glycolipids. *Ann. NY. Acad. Sci.* 605:416–419.
39. Needham, L. K., and R. L. Schnaar. 1991. Adhesion of primary Schwann cells to HNK-1 reactive glycosphingolipids: cellular specificity. *Ann. NY Acad. Sci.* 633:553–555.
40. Needham, L. K., and R. L. Schnaar. 1993. The HNK-1 reactive sulfoglucuronyl glycolipids are ligands for L-selectin and P-selectin, but not E-selectin. *Proc. Natl. Acad. Sci. USA.* 90:1359–1363.
41. O'Shannessy, D. J., H. J. Willison, T. Inuzuka, M. J. Dobersen, and R. H. Quarles. 1985. The species distribution of nervous system antigens that react with anti-myelin-associated glycoprotein antibodies. *J. Neuroimmunol.* 9:255–268.
42. Oulton, M. R., and C. Mezei. 1976. Characterization of myelin of chick sciatic nerve during development. *J. Lipid Res.* 17:167–175.
43. Prasadarao, N., O. Koul, S. A. Tobet, D. K. H. Chou, and F. B. Jungalwala. 1990. Developmental expression of HNK-1 reactive antigens in the rat cerebellum and localization of sulfoglucuronyl glycolipids in molecular layer and deep cerebellar nuclei. *J. Neurochem.* 55:2024–2030.
44. Quarles, R. H. 1989. Human monoclonal antibodies associated with neuropathy. *Methods Enzymol.* 179:291–299.
45. Quarles, R. H., A. A. Ilyas, and H. J. Willison. 1986. Antibodies to glycolipids in demyelinating diseases of the human peripheral nervous system. *Chem. Phys. Lipids.* 42:235–248.
46. Rice, K. G., O. A. Weisz, T. Barthel, R. T. Lee, and Y. C. Lee. 1990. Defined geometry of binding between triantennary glycopeptide and the asialoglycoprotein receptor of rat hepatocytes. *J. Biol. Chem.* 265: 18429–18434.
47. Riopelle, R. J., R. C. McGarry, and J. C. Roder. 1986. Adhesion properties of a neuronal epitope recognized by the monoclonal antibody HNK-1. *Brain Res.* 367:20–25.
48. Sailer, A., and C. Weissmann. 1991. A sensitive and rapid protein assay impervious to detergents. *Technique.* 3:37–38.
49. Scatchard, G. 1949. The attractions of proteins for small molecules and ions. *Ann. NY Acad. Sci.* 51:660–672.
50. Schachner, M. 1989. Families of neural adhesion molecules. *Ciba Found. Symp.* 145:156–172.
51. Schnaar, R. L. 1991. Glycosphingolipids in cell surface recognition. *Glycobiology.* 1:477–485.
52. Smith, P. K., R. I. Krohn, G. T. Hermanson, A. K. Mallia, F. H. Gartner, M. D. Provenzano, E. K. Fujimoto, N. M. Goeke, B. J. Olson, and D. C. Klenk. 1985. Measurement of protein using bicinchoninic acid. *Anal. Biochem.* 150:76–85.
53. Steck, A. J., N. Murray, K. Dellagi, J.-C. Brouet, and M. Seligmann. 1987. Peripheral neuropathy associated with monoclonal IgM autoantibody. *Ann. Neurol.* 22:764–767.
54. Stoolman, L. M. 1989. Adhesion molecules controlling lymphocyte migration. *Cell.* 56:907–910.
55. Svennerholm, L. 1963. Sialic acids and derivatives: estimation by the ion-exchange method. *Methods Enzymol.* 6:459–462.
56. Svennerholm, L., and P. Fredman. 1980. A procedure for the quantitative isolation of brain gangliosides. *Biochim. Biophys. Acta.* 617:97–109.
57. Swank-Hill, P., L. K. Needham, and R. L. Schnaar. 1987. Carbohydrate-specific cell adhesion directly to glycosphingolipids separated on thin-layer chromatography plates. *Anal. Biochem.* 163:27–35.
58. Tiemeyer, M., Y. Yasuda, and R. L. Schnaar. 1989. Ganglioside-specific binding protein on rat brain membranes. *J. Biol. Chem.* 264:1671–1681.
59. Tiemeyer, M., P. Swank-Hill, and R. L. Schnaar. 1990. A membrane receptor for gangliosides is associated with central nervous system myelin. *J. Biol. Chem.* 265:11990–11999.
60. Williams, M. A., and R. H. McCluer. 1980. The use of Sep-Pak C18 cartridges during the isolation of gangliosides. *J. Neurochem.* 35:266–269.
61. Yao, J. K., and G. M. Rastetter. 1985. Microanalysis of complex tissue lipids by high-performance thin-layer chromatography. *Anal. Biochem.* 150:111–116.
62. Yu, R. K., T. Ariga, T. Kohriyama, S. Kusunoki, Y. Maeda, and N. Miyatani. 1990. Autoimmune mechanisms in peripheral neuropathies. *Ann. Neurol.* 27:S30–S35.
63. Zhou, B., S.-C. Li, R. A. Laine, R. T. C. Huang, and Y. T. Li. 1989. Isolation and characterization of ceramide glycanase from the leech, *Macrobdella decora. J. Biol. Chem.* 264:12272–12277.